Weierstraß-Institut
für Angewandte Analysis und Stochastik

im Forschungsverbund Berlin e.V.

Preprint ISSN 0946 – 8633

An iterative method for the multipliers of periodic delay-differential equations and the analysis of a PDE milling model

Oliver Rott[1], Elias Jarlebring[2]

submitted: December 9, 2009

[1] Weierstrass Institute
for Applied Analysis and Stochastics
Mohrenstr. 39
10117 Berlin
Germany
E-Mail: rott@wias-berlin.de

[2] Department of Computer Science
K.U. Leuven
Celestijnenlaan 200 A
3001 Heverlee
Belgium
E-Mail: elias.jarlebring@cs.kuleuven.be

No. 1470
Berlin 2009

2000 *Mathematics Subject Classification.* 47J10, 39A30.

Key words and phrases. Time-periodic delay-differential equations, stability, nonlinear eigenvalue problems.

This article present results of the Belgian Programme on Interuniversity Poles of Attraction, initiated by the Belgian State, Prime Ministers Office for Science, Technology and Culture, the Optimization in Engineering Centre OPTEC of the K.U. Leuven, and the project STRT1-09/33 of the K.U. Leuven Research Foundation. The work of O. Rott was partially supported by the Deutsche Forschungsgemeinschaft, grant SPP1180.

Edited by
Weierstraß-Institut für Angewandte Analysis und Stochastik (WIAS)
Mohrenstraße 39
10117 Berlin
Germany

Fax: + 49 30 2044975
E-Mail: preprint@wias-berlin.de
World Wide Web: http://www.wias-berlin.de/

Abstract. Locally convergent iterative schemes have turned out to be very useful in the analysis of the characteristic roots of delay-differential equations (DDEs) with constant coefficients. In this work we present a locally convergent iterative scheme for the characteristic multipliers of periodic-coefficient DDEs. The method is an adaption of an iterative method called *residual inverse iteration*. The possibility to use this method stems from an observation that the characteristic matrix can be expressed with the fundamental solution of a differential equation. We apply the method to a coupled milling model containing a partial and an ordinary differential equation. The conclusion of the numerical results is that the stability diagram of the coupled model differs significantly from the combined stability diagrams for each subsystem.

1. Introduction

Consider two time-dependent τ-periodic matrices A and B. We will call the equation

$$\dot{x}(t) = A(t)x(t) + B(t)x(t-\tau),\ t \in [s, \infty), \tag{1}$$

where $x(t) \in \mathbb{R}^n$, $\tau > 0$, the associated time-periodic delay-differential equation (TPDDE). We wish to study stability of this equation by computing the (so-called) characteristic multipliers.

There are numerous methods to analyze stability for the special case that A and B are constant. Currently, a two-stage approach is a very common and effective way to compute the multipliers (or the characteristic roots) for the constant-coefficient DDE. The two-stage approach consists of

1) approximating all interesting characteristic roots, and
2) use the approximations as starting guess to local correction method.

The two-stage approach is used in the popular software package DDE-BIFTOOL (see Engelborghs et al. (2002); Samaey et al. (2002)) and also in other contexts, e.g., Gumussoy and Michiels (2009). The first step is typically some form of discretization of an infinite dimensional operator, a linear multistep method in DDE-BIFTOOL, and spectral methods, e.g., Breda et al. (2005), whereas the second step is normally a Newton iteration.

Even though there are several methods (discussed below) which could be used as a first step of the two-stage approach for the more general case (1), there are apparently no local correction schemes in the spirit of the constant-coefficient case. The first contribution of the paper is a correction scheme for the TPDDE. Note also that local correction schemes can be effectively used in combination with continuation methods for stability analysis with respect to uncertainties, which is the application presented in this paper.

We list some methods which could be used as the first step in a two-stage approach. There are methods based on spectral discretization of the monodromy operator (Butcher et al. (2004); Bueler (2007); Breda et al. (2006)), and methods based on discretization and estimating each interval as a constant-coefficient DDE (Insperger and Stépán (2004, 2002a); Insperger (2002); Insperger and Stépán (2002b)) and a collocation discretization combined with a Newton correction is used in Szalai et al. (2006).

Note that even though these methods have been applied successfully to small systems, we expect from the experience with the constant-coefficient case, that a good two-stage approach and in particular an efficient correction scheme is necessary if we wish to treat large systems accurately and reliably.

Models related to milling have been widely studied using TPDDEs. In this work we apply the constructed numerical scheme to such a model and show that the stability diagram changes when the dynamics of the work-piece is taken into account.

These are the main contributions of the paper:

- We observe that a particular formulation of the characteristic equation is a type of problem sometimes called nonlinear eigenvalue problem (in Section 2).
- This observation allows us to adapt a method (residual inverse iteration) and construct an iterative correction method (in Section 3).
- We show the usefulness of the approach by applying it to a milling model coupled with a PDE (in Section 4).
- From the numerical results we establish that other simpler models (involving modelling of the subsystems separately) do not predict the stability diagram accurately.

2. The nonlinear eigenvalue problem for the TPDDE

The stability of TPDDE is traditionally derived from the characteristic roots and multipliers of an infinite dimensional representation in Hale and Verduyn Lunel (1993); Diekmann et al. (1995). We will use a slightly different formulation. Consider the linear time-varying differential equation

$$\dot{p}(t) = C(t, \lambda)p(t), \tag{2}$$

where

$$C(t, \lambda) := A(t) + B(t)e^{-\lambda\tau} - \lambda I. \tag{3}$$

The characteristic roots are those values $\lambda \in \mathbb{C}$ for which the values of p at the boundaries $t = 0$ and $t = \tau$ coincide, i.e., there is a $p(0) = p_0$ such that $p(\tau) = p_0$. The value $\mu = e^{\lambda\tau}$ is called the characteristic multiplier.

Consider the fundamental solution corresponding to (2), i.e., the time-dependent matrix $\Phi(t, \lambda)$ such that $p(t) = \Phi(t, \lambda)p(0)$. The condition $p(\tau) = p(0)$ can now be rewritten as

$$\det\left(\Phi(\lambda) - I\right) = 0, \tag{4}$$

where we have denoted $\Phi(\lambda) = \Phi(\tau, \lambda)$ to stress that $\Phi(\lambda)$ is for a specific time-point.

Note 1. (The constant case). The determinant equation (4) is a generalization of the characteristic equation for the constant case in the following sense. Since C is now constant with respect to t, the fundamental solution of (2) is given by the matrix exponential

$$\Phi(t, \lambda) = \exp(t(A + Be^{-\lambda\tau} - \lambda I)).$$

We insert this into (4) and find that there is a non-zero vector x such that

$$x = \exp(\tau(A + Be^{-\lambda\tau} - \lambda I))x = e^{-\lambda\tau}\exp(\tau(A + Be^{-\lambda\tau}))x,$$

since the identity matrix commutes with any matrix. The spectral mapping principle (see e.g. (Diekmann et al., 1995, Appendix II, Theorem 4.17)) and the fact that $\tau \neq 0$ now implies that

$$(A + Be^{-\lambda\tau})x = \lambda x$$

which is the well known characteristic equation of a DDE with constant coefficients.

3. An adaption of residual inverse iteration

In some contexts, the following class of problems is known as nonlinear eigenvalue problems: find $\lambda \in \mathbb{C}$ and $v \in \mathbb{C}^n \backslash \{0\}$ such that

$$T(\lambda)v = 0. \tag{5}$$

There are numerous methods for nonlinear eigenvalue problems; see, e.g. Mehrmann and Voss (2004); Ruhe (1973).

Clearly, (4) is a nonlinear eigenvalue problem of the form (5). This is a key observation in this work and allows us to solve the problem efficiently. In this work we focus on a method called *residual inverse iteration* (RESINV) introduced in Neumaier (1985). One version of RESINV is the repeated solution of a scalar nonlinear equation, solving a linear system and updating a vector,

$$v_i^T T(\lambda) v_i = 0, \tag{6}$$

$$T(\mu)\Delta v = r_i = T(\lambda_i)v_i \tag{7}$$

$$v_{i+1} = v_i - \Delta v. \tag{8}$$

Note 2. (RESINV vs. Newton). There are Newton methods for the nonlinear eigenvalue problem (5). An important difference between Newton's method and the residual inverse iteration is that the matrix in the linear system $T(\mu)$ does not change throughout the iteration. This will turn out to be advantageous as this is a computationally dominating part of the iteration. The trade-off is that, unlike Newton, residual inverse iteration only has linear convergence (to simple eigenvalues).

3.1. Solving the nonlinear scalar equation.

In the step associated with (6) we need to solve a nonlinear scalar equation to compute $\lambda \in \mathbb{C}$. As usual for nonlinear equations we will solve it with Newton iteration. To this end we have to evaluate

$$f(\lambda) = x^T T(\lambda) x = x^T \Phi(\lambda) x - x^T x \tag{9}$$

$$f'(\lambda) = x^T T'(\lambda) x = x^T \Phi'(\lambda) x \tag{10}$$

for given x. Since $\Phi(\cdot, \lambda)$ is the fundamental solution of (2) with parameter λ, the matrix vector product $\Phi(\tau, \lambda)x = p(\tau, \lambda, x)$ is the solution to (2) with initial condition $p(0) = x$. In order to compute the derivative of $\Phi'(\lambda)x$ we assume p to be sufficiently smooth and form the derivative of (2) with respect to λ

$$\partial_\lambda \partial_t p = \partial_t \partial_\lambda p = \partial_t g = \partial_\lambda C(t, \lambda)p + C(t, \lambda)g, \tag{11}$$

with $g = \partial p / \partial \lambda$. Combining (11) with (2) we obtain the following ODE system

$$\frac{\partial}{\partial t} \begin{bmatrix} p \\ g \end{bmatrix} = \begin{bmatrix} C(t, \lambda) & 0 \\ \partial_\lambda C(t, \lambda) & C(t, \lambda) \end{bmatrix} \begin{bmatrix} p \\ g \end{bmatrix}. \tag{12}$$

In order to find the appropriate initial value for $g(t, \lambda, x, g_0)$, we integrate (2) in time and rearrange the expression to get an explicit formula for the initial condition

$$x = p(t, \lambda) - \int_0^t C(s, \lambda)p(s, \lambda)ds = p(0, \lambda). \tag{13}$$

Since the initial condition x does not depend on λ, the derivative of (13) with respect to λ reads

$$\begin{aligned} 0 &= \partial_\lambda p(t,\lambda) - \int_0^t \partial_\lambda \left(C(s,\lambda)p(s,\lambda)\right) ds \\ &= g(t,\lambda) - \int_0^t \partial_\lambda C(s,\lambda)p(s,\lambda) + C(s,\lambda)g(s,\lambda) ds \\ &= g(0,\lambda), \end{aligned} \tag{14}$$

which can be interpreted as the integral formulation of the second equation in (12). Consequently, (14) provides an expression for the initial condition for the second equation in (12), i.e. $g(0,\lambda) = 0$. Thus, the solution of (12) for initial condition $(x,0)^T$ finally yields $f(\lambda) = x^T p(\tau,\lambda,x) - x^T x$ and $f'(\lambda) = x^T g(\tau,\lambda,x,0)$. For the numerical approximation of the solution of (12) we apply a standard ODE solver, i.e. ode113 (see e.g. Shampine and Gordon (1975)).

3.2. **Evaluating and solving the linear system.** In the second step of RESINV (7) we need to solve a linear system to compute the update of the eigenvector Δv. Since there is no simple closed form for the fundamental solution of (2), we have to approximate the linear operator $T(\mu)$ numerically, preferably again with ode113. Let $\{p^a(t_i,\mu,x)\}$ be an approximate numerical solution of (2) for a discrete time interval $\{t_0,\ldots,t_i,\ldots,\tau\}$, parameter μ and given initial conditions x. Then, the approximate fundamental solution

$$\Phi^a(\tau,\mu) = \left(p^a(\tau,\mu,e_1),\ldots,p^a(\tau,\mu,e_n)\right), \tag{15}$$

can be constructed by solving (2) n-times with different initial conditions e_j, $j = 1,\ldots,n$ and fixed parameter μ. Here, $e_j \in \mathbb{R}^n$ represents the unit vector with component j equal to one. With (4) and (15) we deduce that we can approximate $T(\mu)$ by

$$T^a(\mu) = \Phi^a(\tau,\mu) - I. \tag{16}$$

The residual on the right hand side of (7) can be calculated in the same way as the evaluation of the nonlinear equation (6). In this case we do not need the derivative with respect to λ. Thus, we only have to solve (2) for initial condition $p(0) = v_i$ to end up with the residual

$$r_i(\lambda,v_i) = p^a(\tau,\lambda,v_i) - v_i. \tag{17}$$

Combining (16) and (17) and solving the linear system for Δv_i finally provides the update for the eigenvector. Note that μ is fixed throughout the iteration. Consequently, we have to compute $T^a(\mu)$ only once in each iteration.

3.3. **Algorithmic details.** We describe the RESINV algorithm through the following scheme. Let λ_0 denote the initial guess for the eigenvalue and let v_0 represent the corresponding guess for the eigenvector. During the path following procedures the above values can be taken from the previous solution.

Algorithm 1 RESINV

```
Set RESTOL, μ = λ_0, λ = λ_0 and v = v_0.
Compute T^a(μ) according to (16).
while NOT(stopIter) do
   Solve nonlinear equation (6) to update λ.
   Compute residual r(λ, v) according to (17).
   if |r| < RESTOL then
      stopIter = true
   else
      Solve linear system (7) to get Δv.
      Update v = v − Δv.
   end if
end while
```

4. Modelling and numerical examples

4.1. **Classical 1D system.** As a first example we consider a 1D milling system which has been studied by several authors, see for example Mann et al. (2002) or Butcher et al. (2005). The corresponding equation reads

$$\begin{aligned} &\ddot{y}(t) + 2\zeta\omega_0\dot{y}(t) + \omega_0^2 y(t) \\ &\qquad = -\frac{a_p b(t)}{m}\left(y(t) - y(t-\tau)\right), \end{aligned} \tag{18}$$

$$\begin{aligned} b(t) = \sum_{i=1}^{N} g(\varphi_i(t))\big[&K_t\cos(\varphi_i(t)) \\ &+ K_n\sin(\varphi_i(t))\big]\sin(\varphi_i(t)), \end{aligned} \tag{19}$$

$$\varphi_i(t) = 2\pi\left(nt + (i-1)/N\right), \tag{20}$$

with

$$g(\theta) = \begin{cases} 1 & \text{if } \varphi_s \le P_{2\pi}(\theta) \le \varphi_e \\ 0 & \text{otherwise} \end{cases} \tag{21}$$

where $P_{2\pi}(.)$ denotes the projection of a given angle on the interval $[0, 2\pi]$. The material and cutting parameters have been taken form Butcher et al. (2005) with entry and exit angles $\varphi_s = 0$ and $\varphi_e = \pi$, corresponding to an immersion ration $a/D = 1$.

Equation (18) models the dynamics of a milling process where a rigid cutter machines a rigid workpiece that was mounted on a flexible device. Since this setting exhibits a frequency response function similar to a 1D harmonic oscillator, the stability limits, predicted from the analysis of the 1D system (18), are in perfect agreement with the experimental results (c.f. Mann et al. (2002)). The system has been analyzed for up- and downmilling and different immersion ratios $a/D = 0.25,\ 0.5,\ 0.75,\ 1$, (see Butcher et al. (2005)).

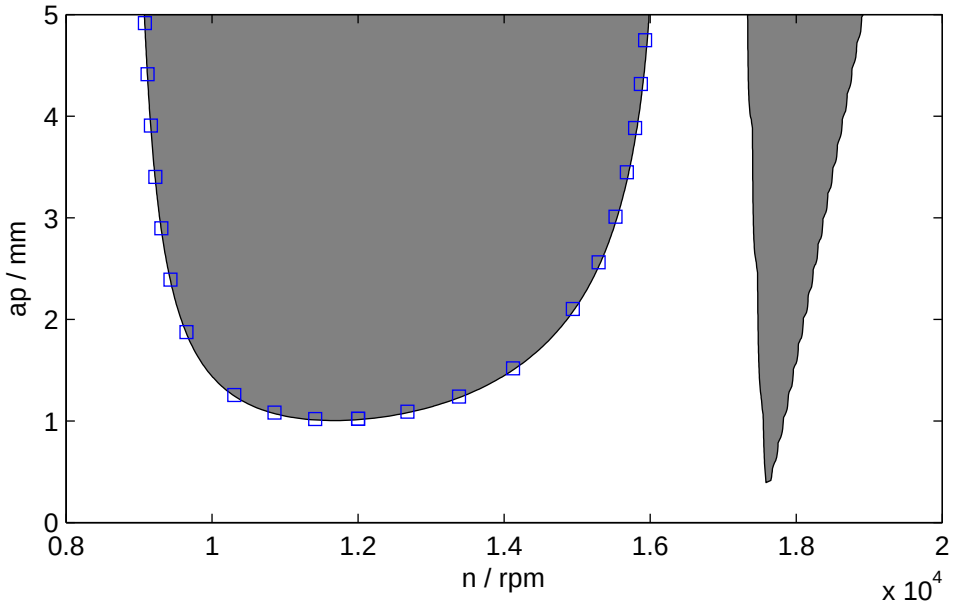

FIGURE 1. Recomputation of the down milling example.

Figure 1 shows the result of the recomputation of the down milling example given in Butcher et al. (2005) for a radial immersion ratio of $a/D = 1$. We combined the method based on RESINV with a simple Euler-Newton continuation method (c.f. Allgower and Georg (1990)) to follow the stability limit given by $\Re(\lambda) = 0$. The result is in perfect agreement with the stability limits obtained with Butchers Chebychev-Collocation-Method, as we see in Figure 1. Note that we cannot follow the stability limit defined by a flip bifurcation, that can be seen in right part of Figure 1. In this case, two conjugate complex eigenvalues become one with vanishing imaginary part when traversing the stability boundary from stable to unstable due to variation of the rotation speed n (see Mann et al. (2003)).

4.2. **A coupled ODE-PDE-system.** Generally, the stability limits for a milling process depend on the cutting forces and on the dynamical characteristics of milling machine and workpiece. ODE-systems derived from modal analysis data provide reliable models for the milling machine and the attached cutter. The workpiece is often assumed to be rigid. However, when machining thin walled pieces the latter assumption eventually leads to large errors in the stability limit prediction. In order to overcome this difficulty, the ODE-system for machine and cutter can be extended by additional equations accounting for the workpiece characteristics that are usually assumed to be constant (see Altintas (2000)). Because of the material removal and since the cutting zone translates along the workpiece boundary, the workpiece characteristics, i.e. the impulse response function, change during the cutting operation. In order to account for these effects, the workpiece has to be considered as series of continuous visco-elastic bodies each being represented by a partial differential equation (c.f. Hömberg and Rott (2008)). The coupling of machine and workpiece representation via the cutting forces, finally leads to a coupled ODE-PDE-system with delay.

Fig 2 shows an example of a simple coupled ODE-PDE-system with delay. While the oscillator on the right represents the rigid milling cutter mounted on a flexible device, the beam on the left is a model for an visco-elastic workpiece. With this example we wish to illustrate the usefulness of the numerical method by analyzing the effect of the coupling. To this end we compare the evolution of the characteristic exponents of the coupled system and

the corresponding decoupled systems. The two decoupled systems can be derived form the equations of the coupled system by the assumptions that either the workpiece is perfectly rigid ((36) and (34)), or that the rigid cutter is mounted on a perfectly ridgid device ((35) and (33)). Note that the assumption that the workpiece is perfectly rigid leads to a system presenting the same structure as (18).

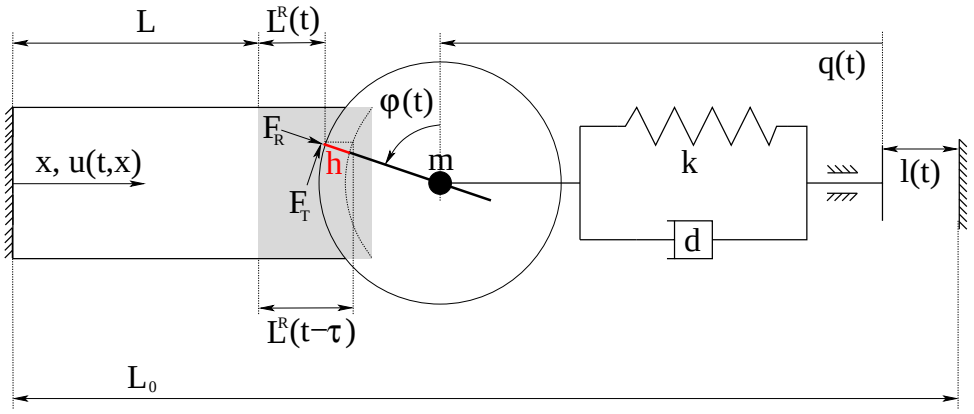

FIGURE 2. Scheme of the coupled ODE-PDE milling model.

The equations of motion for the beam and the rigid cutter mounted on a flexible device read

$$\varrho_0 \, u_{tt}(t,x) - \partial_x \sigma(u(t,x)) = 0, \tag{22}$$

$$u(t,0) = 0, \ \sigma(t,L) = -F/A, \tag{23}$$

$$\ddot{q}(t) + 2\zeta\omega_0 \dot{q}(t) + {\omega_0}^2 q(t) = -F/m, \tag{24}$$

with $\zeta = \frac{d}{2\sqrt{km}}$ and $\omega_0^2 = \frac{k}{m}$. Since we focus on engineering materials we have the following relation for the stress

$$\sigma(u(t,x)) = E\partial_x u(t,x) + D\partial_x u_t(t,x), \tag{25}$$

with E denoting the elastic modulus and D a damping constant corresponding to the Voigt model. The variational form of (22) reads

$$\begin{aligned} &\int_0^L \varrho_0 u_{tt}(t,x)\psi(x)dx + \int_0^L \sigma(u(t,x))\partial_x\psi(x)dx \\ &= \sigma(u(t,L))\psi(L), \forall \psi \in V, \end{aligned} \tag{26}$$

where $V = \{v \in H^1([0,L]), v|_0 = 0\}$. The cutting forces F occurring during the metal cutting process act on the workpiece boundary and on the cutter. The models used to predict the stability limits in milling generally use empirical cutting force models, that can be written as

$$\begin{bmatrix} F_R \\ F_T \end{bmatrix} = \begin{bmatrix} K_R \\ K_T \end{bmatrix} a_p h, \tag{27}$$

to relate the deformations and the resulting forces acting perpendicularly (F_T) and normally (F_R) to the cutting edge, i.e. the tip of the cutter in Figure 2. The above mentioned force F follows from the projection of the vector $(F_R, F_T)^T$ in x-direction, i.e.

$$F(t,h) = g(\varphi(t)) \, (\sin\varphi, \cos\varphi) \, (F_R(h), F_T(h))^T, \tag{28}$$

with g denoting the switch function introduced in (21). Note that, for the sake of simplicity, we focus on milling cutters with only one tooth. In (27) the parameter a_p represents the

axial depth of cut, the vector $(K_R, K_T)^T$ empirical constants and h the uncut chip thickness depending on the deformations of workpiece and cutter. In order to derive a formula for the uncut chip thickness, we consider the beam in Figure 2 that consists of two parts. The first visco-elastic part, of length L, is followed by a small rigid and massless part with varying length $L^R(t)$ that is removed during the cutting operation. From Figure 2 we can derive an explicit formula for this quantity at time t and time $t-\tau$

$$L^R(t) + u(t,L) + L = L_0 - l(t) - \frac{D}{2}\sin\varphi - q(t), \tag{29}$$

$$\begin{aligned} L^R(t-\tau) + u(t-\tau,L) + L &= L_0 - l(t-\tau) \\ &\quad - \frac{D}{2}\sin\varphi - q(t-\tau). \end{aligned} \tag{30}$$

The uncut chip thickness is defined as the difference of $L_R(t-\tau)$ and $L_R(t)$, projected on the vector pointing from the center to the tip of the cutter, i.e.

$$\begin{aligned} h &= \left[(L^R(t-\tau) - L^R(t)\right]\sin\varphi \\ &= f_z \sin\varphi \\ &\quad + \left[u(t,L) - u(t-\tau,L) + q(t) - q(t-\tau)\right]\sin\varphi, \end{aligned} \tag{31}$$

with $f_z = l(t) - l(t-\tau)$ denoting the feed per tooth. Thanks to the above-mentioned expression for the uncut chip thickness, we obtain the following formula for the cutting forces

$$\begin{aligned} F &= g(t)\left(\sin\varphi K_R + \cos\varphi K_T\right) a_p \{[q(t) - q(t-\tau)] \\ &\quad + [u(t,L) - u(t-\tau,L)] + f_z\}\sin\varphi \\ &= a_p w(t)\left[q(t) - q(t-\tau)\right] \\ &\quad + a_p w(t)\left[u(t,L) - u(t-\tau,L)\right] \\ &\quad + \ a_p w(t) f_z \end{aligned} \tag{32}$$

where the function $w(t) := g(t)\left(\sin^2\varphi\ K_R + \cos\varphi\sin\varphi\ K_T\right)$ denotes a τ-periodic coefficient. The last term on the right hand side of (32) represents a periodic perturbation of the system. Since the system is linear, we can split the solution in two parts, i.e $u = u^* + u^p$ and $q = q^* + q^p$, where $u^p(t,x)$ and $q^p(t)$ represent the solution of the system for $F = F^p(t) = a_p w(t) f_z$, that can be considered separately from the stability problem. Thus, the equations determining the stability of the coupled system read

$$\begin{aligned} \int_0^L \varrho_0 u^*_{tt}(t,x)\psi(x)dx + \int_0^L \sigma(u^*(t,x))\partial_x\psi(x)dx \\ = -F^*\psi(L)/A, \quad \forall\psi \in V, \end{aligned} \tag{33}$$

$$\ddot{q}^*(t) + 2\zeta\omega_0\dot{q}^*(t) + {\omega_0}^2 q^*(t) = -\frac{F^*}{m}, \tag{34}$$

$$\begin{aligned} F^* = \ & a_p w(t)\left[q^*(t) - q^*(t-\tau)\right] \\ & + a_p w(t)\left[u^*(t,L) - u^*(t-\tau,L)\right]. \end{aligned}$$

Note that, setting the feed per tooth $f_z = 0$ in (32) yields the same system as above for nonzero feed. In order to solve the system (33)- (34) numerically, we apply the Garlerkin method for $u(t,x)$ and approximate the basis of $H^1([0,L])$ with linear finite elements. The resulting space discrete system has the same form as (1), if we introduce additional variables to obtain a first order equation in time.

Now we can use the path following algorithm to determine the stability limits of the coupled system. The material and cutting parameters are $m = 0.06\ kg$, $\zeta = 1.2\ \%$, $\omega_0 = 2\pi \times 2241.49\ Hz$, $N = 1$, $K_n = 690.0\ N/mm^2$ and $K_t = 894.0\ N/mm^2$. The entry and exit angles have been chosen as $\varphi_s = 0$ and $\varphi_e = \pi$. The material parameters for the beam equation have been set to $\rho = 0.27\ kg/mm^3$, $E = 70 \times 10^4\ kg/(sec^2 mm)$, $D = 0.0378\ kg/(mmsec)$, $L = 0.1\ mm$ and $A = 10\ mm^2$. The beam was discretised with 5 elements. Note that the beam parameters are artificial values that have been chosen for presentation purposes. Figure 3 shows the result of the path following procedure.

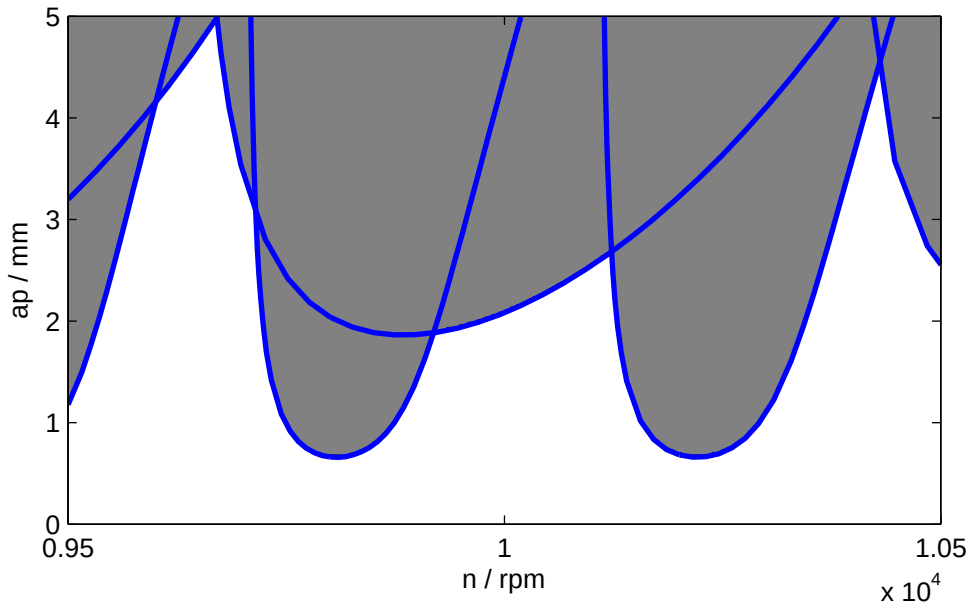

FIGURE 3. Stability chart for the coupled system (grey shaded area represents the unstable regions).

As in section 4.1 the white region characterises the combinations of ap and n where the solution of the coupled system is asymptotically stable. The blue lines show the evolution of the paths defined by $\Re(\lambda(n, a_p)) = 0$.

Next, we focus on the effect of the coupling. To this end, we simplify the coupled system. As mentioned before, we neglect either the second or the first part of the cutting force in (33) and (34). Thus, the force F^* can be written as

$$F^* \approx F^*_{pde} = a_p w(t) \left[u^*(t, L) - u^*(t - \tau, L)\right], \tag{35}$$

$$F^* \approx F^*_{ode} = a_p w(t) \left[q^*(t) - q^*(t - \tau)\right]. \tag{36}$$

Using (35) for the right hand side of (33) and (36) for (34) leads to a decoupling of the system and the path following can be carried out for each equation separately. The comparison of the corresponding stability lobes reveals the effect of the coupling. In Figure 4 the red

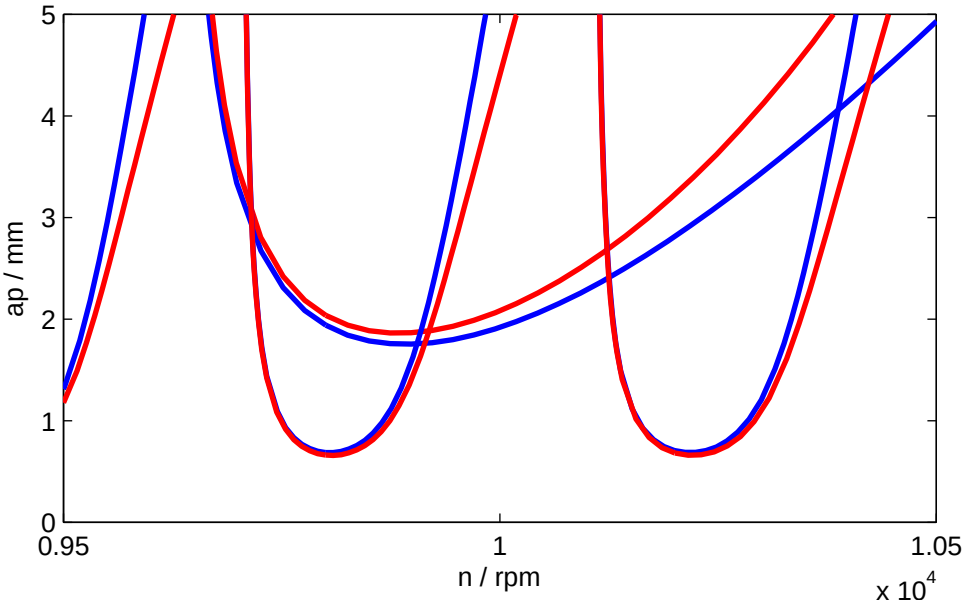

FIGURE 4. Comparison of the coupled (red lines) system and decoupled (blue lines) systems.

lines represent the stability lobes corresponding to the coupled system. The result of the computations for the decoupled system has been plotted with blue lines. The main differences between the blue and the red lines occur in the right part of each stability lobe. While the lobe corresponding to an eigenvalue of the oscillator equation lies below the lobe of the coupled system, the stability limit corresponding to an eigenvalue of the beam equation is higher than the respective curve for the coupled system.

Since we approximate the space continuous beam equation with finite elements, we introduce an additional discretization error. In order to display the effect of the discretization we focus on the stability lobe that has a minimum at $n = 9800\ rpm$, c.f. Figure 3. We discretise the beam equation with 5, 10 and 20 elements and recompute the stability lobe for each grid size. In Figure 5 we observe that the stability lobe moves to the left for smaller grid sizes. In order to explain this observation, we recall that the finite element approximation leads to an overestimation of the first eigenfrequency of the continuous beam equation. The refinement of the grid reduces the approximation error and the lowest eigenfrequency converges to the value of the continuous system. Since the position of the stability lobe is determined by one of the eigenfrequencies of the oscillation system, the lobe translates because of the better approximation of the first eigenfrequency of the beam equation.

Finally, we conclude that the path following method based on the RESINV algorithm can be used to analyse the stability of coupled ODE-PDE-systems. We have shown that stability limits of the coupled system differ from the stability limits of the corresponding decoupled systems. The most significant discrepancy can be noticed on the right part of each lobe. Thus, the disregard of structural components during the modeling of a milling system may lead to errors in the prediction of the stability limits. The finite element approximation of

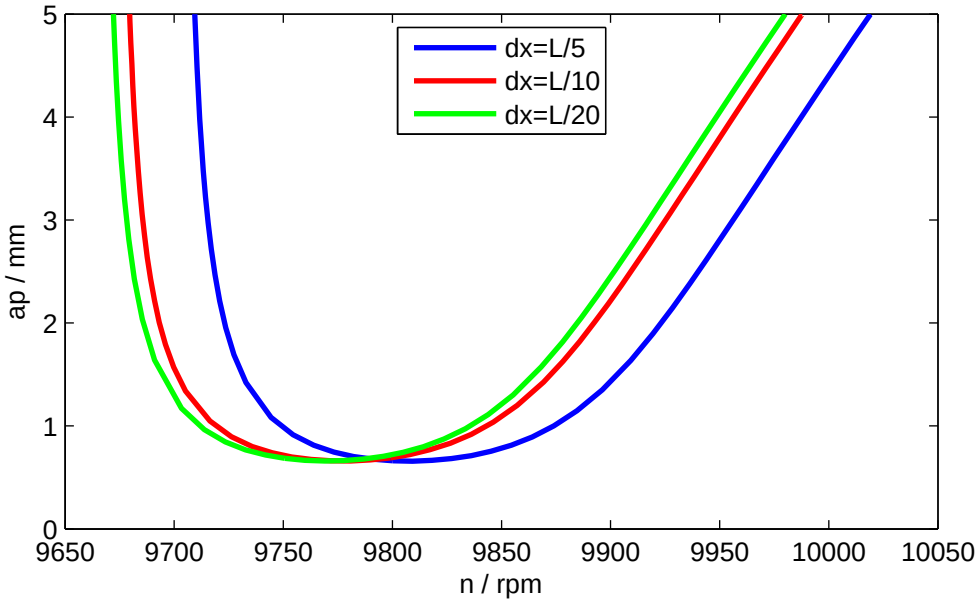

FIGURE 5. Convergence of the stability lobe.

the PDE-part causes further errors in the prediction of the stability limits. The stability lobes translate with decreasing grid size in the direction of lower values of n.

5. Conclusions and outlook

In this paper we have presented a numerical linear algebra approach to the characteristic roots of time-periodic delay-differential equations, in the sense that we have adapted a method from the field of nonlinear eigenvalue problems to construct an iterative correction scheme.

Although we have focused on the method residual inverse iteration, many of the methods reviewed in Ruhe (1973); Mehrmann and Voss (2004), could be applied to the implicitly stated nonlinear eigenvalue problem (4). We have chosen RESINV as we can implement it in a way where we only compute one matrix. Finally, the choice of the generality setting is done to keep the presentation simple. The general methodology is apparently applicable to more general problems such as systems with multiple delays and cases where the delay does not coincide with the period. These type of systems are necessary in more accurate milling models.

References

Allgower, E. and Georg, K. (1990). *Numerical Continuation Methods*. Springer-Verlag.

Altintas, Y. (2000). *Manufacturing Automation*. Cambridge University Press.

Breda, D., Maset, S., and Vermiglio, R. (2005). Pseudospectral differencing methods for characteristic roots of delay differential equations. *SIAM J. Sci. Comput.*, 27(2), 482–495.

Breda, D., Maset, S., and Vermiglio, R. (2006). Numerical computation of characteristic multipliers for linear time periodic coefficients delay differential equations. In *Proceedings of the Sixth IFAC Workshop on Time-Delay Systems, L'Aquila, Italy*.

Bueler, E. (2007). Error bounds for approximate eigenvalues of periodic-coefficient linear delay differential equations. *SIAM J. Numer. Anal.*, 45(6), 2510–2536.

Butcher, E.A., Ma, H., Bueler, E., Averina, V., and Szabo, Z. (2004). Stability of linear time-periodic delay-differential equations via Chebyshev polynomials. *Int. J. Numer. Methods Eng.*, 59(7), 895–922.

Butcher, E., Nindujarla, P., and Bueler, E. (2005). Stability of up- and down-milling using Chebyshev collocation method. In *Proceedings of IDETC/CIE 2005*.

Diekmann, O., van Gils, S.A., Verduyn Lunel, S.M., and Walther, H.O. (1995). *Delay equations. Functional-, complex-, and nonlinear analysis*. Applied Mathematical Sciences. 110. New York, NY: Springer-Verlag.

Engelborghs, K., Luzyanina, T., and Roose, D. (2002). Numerical bifurcation analysis of delay differential equations using DDE-BIFTOOL. *ACM Transactions on Mathematical Software*, 28(1), 1–24.

Gumussoy, S. and Michiels, W. (2009). Computing $\mathcal{H}_\infty$ norms of time-delay systems. In *Proceed ings of the 48th IEEE Conference on Decision and Control*.

Hale, J. and Verduyn Lunel, S.M. (1993). *Introduction to functional differential equations*. Springer-Verlag.

Hömberg, D. and Rott, O. (2008). Modelling, analysis and stability of milling processes including workpiece effects. In *Proceedings of ECMI 2008 (to appear)*.

Insperger, T. (2002). *Stability analysis of periodic delay-differential equations modeling machine tool chatter*. Ph.D. thesis, Budapest University of Technology and Economics.

Insperger, T. and Stépán, G. (2002a). Semi-discretization method for delayed systems. *Int. J. Numer. Methods Eng.*, 55(5), 503–518.

Insperger, T. and Stépán, G. (2002b). Stability chart for the delayed Mathieu equation. *Proc. R. Soc. Lond., Ser. A, Math. Phys. Eng. Sci.*, 458(2024), 1989–1998.

Insperger, T. and Stépán, G. (2004). Updated semi-discretization method for periodic delay-differential equations with discrete delay. *Int. J. Numer. Methods Eng.*, 61(1), 117–141.

Mann, B., Insperger, T., Bayly, P., and Stépán, G. (2003). Stability of up-milling and down-milling, part 2: experimental verification. *International Journal of Machine Tools and Manufacture*, 43, 3540.

Mann, B., Insperger, T., Bayly, P., Stépán, G., Schmitz, T., and Peters, D. (2002). Effects of radial immersion and cutting direction on chatter instability in end-milling. In *Proceedings of IMECE02*.

Mehrmann, V. and Voss, H. (2004). Nonlinear eigenvalue problems: A challenge for modern eigenvalue methods. *GAMM Mitteilungen*, 27, 121–152.

Neumaier, A. (1985). Residual inverse iteration for the nonlinear eigenvalue problem. *SIAM J. Numer. Anal.*, 22, 914–923.

Ruhe, A. (1973). Algorithms for the nonlinear eigenvalue problem. *SIAM J. Numer. Anal.*, 10, 674–689.

Samaey, G., Engelborghs, K., and Roose, D. (2002). Numerical computation of connecting orbits in delay differential equations. *Numer. Algorithms*, 30, 335–352.

Shampine, L.F. and Gordon, M.K. (1975). *Computer Solution of Ordinary Differential Equations*. W. H. Freeman, San Francisco.

Szalai, R., Stépán, G., and Hogan, J. (2006). Continuation of bifurcations in periodic delay-differential equations using characteristic matrices. *SIAM J. Sci. Comput.*, 28(4), 1301–1317.